

appear on the $m^*(D)$ or $m^*(p_s)$ curve.

We note that although the linear impedance of the plate in an oblique field also has a singularity upon satisfaction of the conditions (48) with odd l ^[11]; however, the singularity here is very weak. The resonance contribution to the impedance is proportional to the square of the small parameter $\delta/r\varphi$, where φ is the angle of inclination of the magnetic field to the surface of the plate.^[11] In thin plates, this contribution also contains an additional small parameter. Therefore, the singularities of the surface impedance at frequencies determined from (48) at odd l have not been observed experimentally to date. Of course, the dimensional nonlinear cyclotron resonance in an oblique field gives more detailed information on the electron spectrum than does the linear case.

Consideration of the problem of the nonlinear cyclotron resonance in a plate in the case in which reflection of the electrons from the boundary is not close to specular can be carried out if we use the results obtained above. This is to be the object of a separate investigation. Here we only note that the odd nonlinear resonance has a logarithmic character and at even l the singularity can become stronger if the parameter $\omega\tau$ is sufficiently large.

- ¹N. Bloembergen, R. K. Chang, S. S. Iha, and C. H. Lee, *Phys. Rev.* **174**, 813 (1968).
- ²G. I. Leviev and E. G. Yashin, *Pis'ma Zh. Eksp. Teor. Fiz.* **10**, 257 (1969) [*JETP Lett.* **10**, 163 (1969)].
- ³G. I. Leviev, *Fiz. Tverd. Tela (Leningrad)* **12**, 2131 (1970) [*Sov. Phys. Solid State* **12**, 1691 (1971)].
- ⁴R. T. Bate and W. R. Wisseman, *Phys. Rev.* **181**, 763 (1969).
- ⁵M. Ya. Azbel' and L. B. Dubovskii, *Pis'ma Zh. Eksp. Teor. Fiz.* **5**, 414 (1967) [*JETP Lett.* **5**, 338 (1967)].
- ⁶M. Ya. Azbel' and E. A. Kaner, *Zh. Eksp. Teor. Fiz.* **32**, 896 (1957) [*Sov. Phys. JETP* **730** (1957)]; *Phys. Chem. Sol.* **6**, 113 (1958).
- ⁷R. Chambers, in the collection *Fizika metallov (Physics of Metals)*, vol. 1: *Electrons*, (J. Ziman, ed.) Mir, 1972.
- ⁸A. P. Volodin, M. S. Khaikin, and V. S. Edel'man, *Pis'ma Zh. Eksp. Teor. Fiz.* **17**, 491 (1973) [*JETP Lett.* **17**, 353 (1973)]; *Zh. Eksp. Teor. Fiz.* **65**, 2105 (1973) [*Sov. Phys. JETP* **38**, 1052 (1074)].
- ⁹A. P. Volodin and M. S. Khaikin, *Zh. Eksp. Teor. Fiz.* **70**, 2006 (1976) [*Sov. Phys. JETP* **43**, 1046 (1976)].
- ¹⁰M. A. Lur'e and V. G. Peschanskiĭ, *Zh. Eksp. Teor. Fiz.* **66**, 240 (1974) [*Sov. Phys. JETP* **39**, 114 (1974)].
- ¹¹M. A. Lur'e and V. G. Peschanskiĭ, *Fiz. Nizk. Temp.* **1**, 1044 (1975) [*Sov. J. Low Temp. Phys.* **1**, 502 (1975)].
- ¹²O. V. Kirichenko, M. A. Lur'e, and V. G. Peschanskiĭ, *Zh. Eksp. Teor. Fiz.* **70**, 337 (1975) [*Sov. Phys. JETP* **43**, 175 (1975)].

Translated by R. T. Beyer

Amplification and generation of coherent phonons in ruby under conditions of spin-level population inversion

E. M. Ganapol'skiĭ and D. N. Makovitskiĭ

Institute of Radiophysics and Electronics, Ukrainian Academy of Sciences

(Submitted April 10, 1976)

Zh. Eksp. Teor. Fiz. **72**, 203–217 (January 1977)

The processes of amplification and generation of coherent phonons in ruby at a frequency 9.12 GHz following inversion of the spin-level populations by electromagnetic pumping at 23 GHz were investigated at temperatures 1.7–4.2°K. The resonant-longitudinal-phonon lifetime estimated from the threshold the gain of the hypersound excited in a crystal is $\tau_{ph} \approx 2 \times 10^{-5}$ sec. A nonstationary effect, wherein the hypersound gain increases appreciably under conditions when the pump line is saturated on the wing is observed. This effect is interpreted on the basis of the thermodynamics of an electron-nuclear system made up of the Zeeman and dipole pools of the Cr^{3+} ions and the Zeeman pool of the Al^{27} nuclei. Stationary incoherent emission of phonons is realized. It is shown that the multimode character of this emission at the natural frequencies of the acoustic resonance and the narrow spectral radiation interval are due to the fact that phonon generation takes place under conditions of spatial disequilibrium in the case of a small excess above the pump threshold.

PACS numbers: 78.60.Mq

1. INTRODUCTION

In connection with the successful use of hypersound waves in solid-state investigations, interest in the amplification and generation of these waves has greatly increased recently. Particular attention, however, has been paid to amplification under conditions of carrier drift in semiconductors, while amplification and generation of hypersonic waves based on stimulated emission by impurity paramagnetic centers in crystals have been

practically neglected. The gist of these effects, predicted back in the early sixties independently by Townes,^[1] Kopvillem and Korepanov,^[2] and Kittel,^[3] consists in the following:

A hypersonic wave in a crystal with nonmagnetic centers is resonantly absorbed, owing to the electron-phonon coupling, when the quantum of the elastic oscillations of the waves is equal to the spacing between the energy levels of the center in the magnetic field. If the

populations of these levels are inverted, then the hypersonic wave is amplified rather than absorbed. If the gain is large enough, exceeding the losses in the crystal, self-excitation of the hypersound becomes possible, i. e., the conversion of incoherent photons corresponding to thermodynamic equilibrium into monochromatic elastic oscillations or into oscillations with a discrete spectrum.

This phenomenon is similar to the well known laser effect and can be called in analogy the phaser effect. The phaser effect was detected by Tucker, who observed both amplification^[4] and generation^[5] of phonons following inversion of the populations of the spin levels of Cr³⁺ in ruby. Under analogous conditions, Peterson and Jacobsen^[6] have registered phonon amplification for Ni²⁺ centers in corundum, but no generation was observed, although the gain, according to their data^[6] exceeded the losses in the crystal. The results of these investigations, obtained with imperfect hypersonic experimental techniques, constituted the bulk of the experimental data on the phaser effect.

Since amplification is observed in the inverted system, it is of interest to ascertain whether it is possible to obtain in such a system stationary coherent phonon generation in analogy with cw lasers. The results obtained by Tucker,^[5] who observed unstable oscillations at the noise level, did not make it possible to answer this question in the affirmative, all the more since maser experiments have shown that the inverted paramagnetic system of ruby is capable of generating nonstationary oscillations with a wide spectrum.^[7,8]

The definite progress made in the field of excitation and reception of hypersonic waves in recent years makes a thorough study of the phaser effect possible. We report here results^[1] of an experimental investigation of the amplification and generation of hypersound in ruby following inversion of the spin-level populations by electromagnetic pumping. The amplification effect was investigated both in a stationary regime and in a nonstationary regime, under conditions when the frequencies of the signal and the pump were and were not identical with the corresponding frequencies of the resonant transitions. In the nonstationary regime, an increase of the gain of the hypersound at large detunings was observed. The nature of this effect, in which, as it turned out, the behavior of the electron spin system of Cr³⁺ is strongly influenced by the magnetic Al²⁷ nuclei contained in the ruby crystal matrix, is explained. Stationary coherent emission of phonons is realized and its mechanism is explained. It is established that the multifrequency character of this radiation is due to the spatial disequilibrium, wherein the substantial inhomogeneity of the elastic field of the natural modes of the phaser acoustic resonator causes the production of a number of independent self-oscillating systems corresponding to different modes and generating simultaneously at different frequencies.

2. FEATURES OF THE EXPERIMENTAL PROCEDURE

Phaser effects were investigated in ruby at low frequencies 1.7–4.2 °K with the crystal pumped by a

23-GHz electromagnetic field. X-band hypersonic waves were used to measure the gain. To investigate the effects, the setup illustrated schematically in Fig. 1 was developed. Its principal elements are a ruby acoustic resonator (5), a hypersonic converter with electrodynamic system to match it to the transmission waveguide line (6, 7, 8), and an electromagnetic-field resonator (4) to pump the spin levels of the ruby.

The acoustic resonator 5 was made of ruby grown by the Verneuil method and cut to form a round rod of 2.6 mm diameter and 17.6 mm length. Its geometrical axis coincided within 1° with the crystallographic threefold symmetry axis. The end faces of the resonator rod 5 were optically flat and parallel (the surface roughnesses did not exceed 0.05 μ, and deviation from parallelism was less than 1"). The material used for the acoustic resonator contained a relatively small number of defects that influenced the electronic spectrum of the Cr³⁺ impurity centers and the hypersound absorption. Preliminary measurements by the ESR methods have shown that in this material, with a Cr³⁺ concentration 0.28 at.%, the width of the resonance line in the signal transition under conditions of a symmetrical level scheme is 65 MHz. The acoustic properties of the resonator were determined at T = 4.2 °K by recording the hypersound resonances as the frequency of the continuous hypersound signal was swept in the vicinity of 9.12 GHz. The hypersound resonances correspond to axial modes of the longitudinal oscillations and are spaced by equal frequency intervals of 310 kHz.

To excite in the rod a pure longitudinal hypersonic wave along a threefold axis, a piezoelectric ZnO film of 0.35 μ thickness on an aluminum sublayer 0.15 μ thick were deposited on one of its ends by vacuum evaporation. The film together with the electrodynamic system served to convert^[11] the electromagnetic wave into a hypersound wave. The same film, by virtue of the reversibility of the piezoelectric effect, converted the hypersound oscillations in the rod into the field of an electromagnetic wave.

The electrodynamic system of the converter contains a molybdenum disk with a conical aperture, through which a thin molybdenum conductor passes through a glass seal. The end face of the conductor is flush with the surface of the disk and is ground and polished, together with this surface and the glass insulator, to the

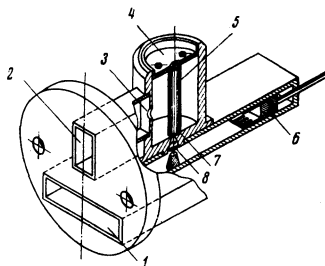


FIG. 1. Phaser arrangement: 1—signal waveguide, 2—pump waveguide, 3—coupling port, 4—electromagnetic pump cavity, 5—acoustic resonator, 6—waveguide plunger, 7—piezoelectric film, 8—conical junction.

same accuracy as the end faces of the acoustic resonator. The end face with the ZnO film was in direct contact with the molybdenum disk.

The hypersound converter was matched to the transmission line (waveguide) with a coaxial-waveguide junction (Fig. 1) containing a conical junction and a waveguide plunger, as well as inductive and capacitive matching elements not shown in Fig. 1. The electromagnetic wave excites in the ZnO film an electric field that is concentrated in a small region adjacent to the end face of a thin conductor sealed into the disk. This region (disk of 0.5 mm diameter and 0.35 μ height) serves as the antenna to transmit and receive the hypersound wave in the ruby crystal. Because of the high electric-field concentration, this converter is highly efficient. The loss to the double conversion does not exceed 30 dB in a frequency band of approximately 100 MHz.

The acoustic resonator is placed in the electromagnetic pump resonator. The pump resonator is cylindrical, of type H_{011} (magnetic field antinode along the axis). The coupling of the resonator with the waveguide is diffractive, through an opening in the side wall. At temperatures 1.7–4.2°K, the loaded Q of the pump resonator with the ruby rod was 10^4 .

To measure the resonant absorption and amplification of the hypersound we used the standard echo-pulse method. The pulse duration was 0.5–1 μ sec, and the pulse repetition frequency ranged from 300 Hz to 10 kHz. These measurements were performed in a linear regime, at a low intensity of the hypersonic wave, when no effects of the saturation of the signal transition by hypersound manifest themselves. To investigate the spectral composition of the stimulated hypersound radiation, when working in the generation regime, we used an X-band spectrum analyzer with a resolution of 20 kHz.

3. AMPLIFICATION OF THE HYPERSOUND

The investigation of the amplification and of the generation (Sec. 5) was carried out mainly under conditions where the spin-level scheme of the impurity Cr^{3+} ions was symmetrical, when the magnetic field H was directed at an angle $\theta = \theta_0 = 54^\circ 44'$ to the trigonal axis of the crystal. In this case, as is well known, the pumping efficiency is maximal for the transitions 1–3 and 2–4 (the levels are numbered in order of increasing energy). The gain is the result of induced transitions between levels 2 and 3 when the longitudinal hypersonic wave propagating along the trigonal axis interacts with the spin system of the Cr^{3+} in the ruby. According to data obtained by the acoustic paramagnetic resonance method,^[12] the matrix element of this interaction, which depends on θ , has an obtuse maximum at $\theta \approx \theta_0$. In addition, in a symmetrical level scheme, i.e., in the case of push-pull pumping, the inversion coefficient necessary for the investigation of the gain in the below-threshold regime and to attain the generation regime can become relatively large.

With increasing pump power delivered to the resonator with the crystal, the resonant absorption of the hypersonic wave in the crystal gives way to amplification.

The amplification manifests itself in a decrease of the total hypersound absorption coefficient α , and is accompanied by an appreciable increase of the number of observed hypersound echo signals (Fig. 2).

Using the known expressions for the coefficient of resonant hypersound absorption^[13] and taking into account the inversion of the populations of levels 2 and 3, we can write the expression for α in the form

$$\alpha = \alpha_n - \alpha = \alpha_n - I \frac{2\pi^2 (\nu^s)^2 [g(\nu^s)]^2 N F_{32}^2}{(2S+1) \rho v^3 k_B T}, \quad (1)$$

where α_n is the coefficient of the nonresonant losses of the hypersound (in the absence of a magnetic field), α is the gain of the hypersound, I is the inversion coefficient, ν^s is the frequency of the hypersound signal, $g(\nu^s)$ is the line shape of the acoustic paramagnetic resonance with the signal transition, N is the concentration of the active paramagnetic ions, S is the spin of the ion, ρ is the density of the crystal, v is the propagation velocity of the signal hypersound wave, k_B is Boltzmann's constant, T is the temperature, $F_{32} = |\langle \psi_3 | \frac{1}{2} G_{33} (3S_z^2 - S(S+1)) | \psi_2 \rangle|$ is the modulus of the matrix element of the spin-phonon interaction Hamiltonian,^[12] G_{33} is the component of the spin-phonon interaction tensor, $|\psi_2\rangle$ and $|\psi_3\rangle$ are the wave func-

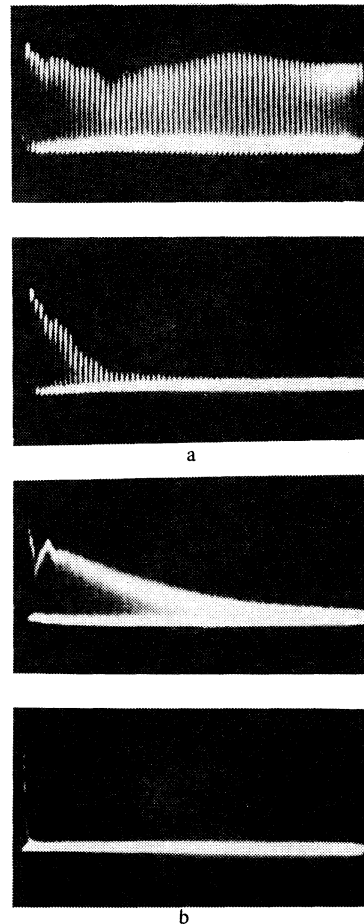


FIG. 2. Amplification of hypersound following inversion of the populations of the spin levels in ruby. Sequences of hypersound echo pulses obtained in the amplification regime (upper oscillograms) and without amplification (lower oscillograms). Sweep duration: 200 μ sec (a) and 2 msec (b).

tions belonging to the levels of the signal transition,^[14] and S_z is the operator of spin projection on the z axis, which coincides with the trigonal axis of the crystal.

The values of α measured in the pulsed regime^[2] agree well with (1). Under conditions when the pump transitions are fully saturated in a resonant field $H_0^p = 3920$ Oe, the hypersound gain is 0.6 dB/cm at 1.7°K and decreases monotonically, $\propto T^{-1}$, when the temperature is increased to 4.2°K. Substitution in (1) of the values $I = 3.3$,^[15] $\nu_0^s = 9.12$ GHz, $g(\nu_0^s) = 10^{-8}$ Hz⁻¹, $N = 1.3 \cdot 10^{19}$ cm⁻³, $S = \frac{3}{2}$, $\rho = 4$ g/cm³, $v = 1.085$ cm/sec, $T = 1.7$ °K, and $F_{32} = 5$ cm⁻¹^[12] yields $\alpha = 0.62$ dB/cm.

We measured also the frequency dependences of the gain. In these measurements, the angle θ and the magnetic field were fixed: $\theta = \theta_0$ and $H = 3920$ Oe. At a small acoustic length l , when $\alpha l < 1$, the gain bandwidth is close, in accordance with (1), to the width of the signal transition, approximately 65 MHz. With increasing l , i. e., in the case of multiple reflection of the hypersound beam from the ends of the rod, a noticeable narrowing of the amplification band is observed, due to the same causes as in ordinary electromagnetic traveling-wave masers,^[15] for under our conditions the amplification of the hypersound takes place in fact in a traveling-wave regime (the relation $\tau v < l_0 \ll l$ is satisfied).

With increasing hypersound intensity, the gain decreases because of the saturation of the signal transition. At a pulse duration 1 μ sec and a repetition frequency 10 kHz, the saturating intensity of the hypersound is ≈ 2 mW/cm².

By increasing the pump power or by lowering the temperature (in the absence of a saturation margin for the pump transitions) it is possible to obtain a below-threshold regime in which $\alpha \approx \alpha_n$ and the total absorption α_v is quite small. In this case the hypersound pulse stays in the crystal for a long time and experiences numerous reflections from the end faces. The oscillograms of Fig. 2 correspond in fact to the pre-threshold regime. We see here a sequence containing more than 600 hypersound echo pulses, corresponding to a hypersound-pulse lifetime on the order of 2 msec. From this we can determine the absolute magnitude of the nonresonant absorption of the hypersound. It should be noted that the ordinary echo-pulse method does not make it possible to measure the nonresonant-loss coefficient α_n at low temperatures. This quantity is usually determined as a measure of the monotonic decrease of the amplitude of the echo signals with decreasing acoustic-path length. At low temperatures, however, α_n is quite small and the decrease of the echo pulses is not monotonic. It is determined principally not by the absorption of the hypersound in the sample, but by the distortion of the phase front of the hypersound wave in reflections from the boundaries of the sample and by scattering from the defects of the crystal structure.

Measurements of the gain in the subthreshold regime have shown that $\alpha_n \lesssim 0.2$ dB/cm at $T = 4.2$ °K. From this we can find that the lifetime of the resonant longitudinal phonons in the acoustic resonator is $\tau_{ph} \gtrsim 2$

$\times 10^{-5}$ sec. The ultrasound losses that give rise to τ_{ph} are connected with absorption in the volume of the crystal and in the converter, which is in good acoustic contact with the crystal, and also with the escape of the phonons to the helium reservoir. Therefore the obtained time τ_{ph} can characterize only the lower limit of the lifetimes of the resonant phonons in ruby at low temperatures.

It is important to note that even this lower limit τ_{ph} , obtained directly from the value of the threshold gain, exceeds by more than two orders of magnitude the lifetime of the resonant phonons with which one usually deals in the interpretation of experiments on paramagnetic relaxation under conditions of the phonon bottleneck, where it is assumed that $\tau_{ph} \approx l'/2v$ (l' is the characteristic dimension of the crystal, and at $l' = 0.1$ cm we obtain $\tau_{ph} \approx 10^{-7}$ sec).^[16] This circumstance points to the need of reviewing the existing notions concerning the single-phonon process of paramagnetic relaxation at low temperatures.

4. NONSTATIONARY EFFECT IN HYPERSOUND AMPLIFICATION

1. The value of the gain in the nonstationary region (Sec. 3) depends only on the modulus of the detuning $\Delta\nu^s = \nu^s - \nu_0^s$ of the signal frequency ν^s relative to the quantity ν_0^s corresponding to the splitting of the signal levels (2, 3) in the resonant pump field H_0^p , and decreases rapidly with increasing $|\Delta\nu^s|$. The stationary characteristics of the gain are preserved also in the case of slow variation of the magnetic field in the vicinity of the signal resonance, at a rate $|\partial H/\partial t| \lesssim 2-3$ Oe/sec.

In the case of fast variation of the magnetic field with $|\partial H/\partial t| \approx 20-200$ Oe/sec, a nonstationary effect was observed, consisting of an appreciable increase of the hypersound gain α (at large detunings of the signal frequency) in comparison with the stationary value of α (at the same values of the detuning). Quantities pertaining to the stationary and nonstationary regimes will be labeled "st" and "ns," respectively.

The conditions for the appearance of the nonstationary effect are shown in Fig. 3. Let the signal frequency ν^s deviate from ν_0^s in such a way that $\Delta\nu^s < 0$. The effect appears if the initial value of the magnetic field is set at a point $H^b > H_0^p$, and then the field is rapidly decreased and passes through the resonant pump and signal region. If the sign of the detuning is reversed, i. e., if $\Delta\nu^s > 0$, the "correct" preliminary setting of the field needed for the effect to appear is reversed: $H^b < H_0^p$. In this case an increase of the gain in comparison with the stationary regime takes place if the field is rapidly increased and passes through the resonance region of the pump and of the corresponding signal. In both cases, the condition for the realization of the nonstationary effect is that after setting the field at the point H^b (at which point the field must remain fixed for a time on the order of 10 sec or more), the passage through the region of the pump line width is fast and precedes the passage through the signal line, when the gain is registered. Getting ahead of ourselves, we in-

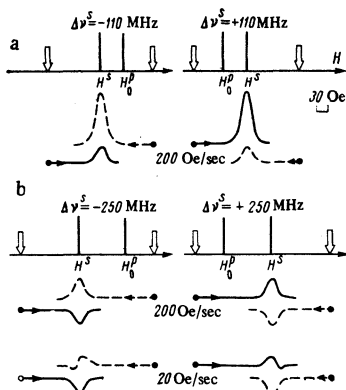


FIG. 3. Amplification of hypersound in nonstationary regime. The numbers next to the resonance curves $\alpha(H)$ indicate the rate of passage of the magnetic field $|\partial H/\partial t|$. The solid and dashed curves were obtained at $\partial H/\partial t > 0$ and $\partial H/\partial t < 0$, respectively. The light arrows indicate the positions of the points H^b , at which the magnetic field was fixed for a time ≈ 10 sec prior to the start of the passage. The signal frequency detuning is $\Delta\nu^s = \pm 110$ MHz (a) and $\Delta\nu^s = \pm 250$ MHz (b).

indicate that fast passage through the region of the peak of the pump line is the cause of the effect, whereas fast passage through the signal region is needed only to have time to register the effect.

The most typical experimental data, obtained at $T = 4.2$ K, $H_0^p = 3920$ Oe (corresponding to $\nu_0^p = 23$ GHz), $\theta = \theta_0$, and a pump-field intensity in the sample $2H_1 = 0.5$ Oe (which provides a margin of more than 20 dB for saturation of the pump transitions when the pump line is saturated at the center) are shown in Figs. 3 and 4.

We consider first the case of a detuning $\Delta\nu^s = -110$ MHz (Fig. 3a, on the left). The resonance of the signal H^s is shifted relative to the resonance of the pump H_0^p towards weaker fields—and accordingly an increase of the magnetic field in the nonstationary regime ($|\partial H/\partial t| = 200$ Oe/sec) yields practically the same gain (solid line) as in the stationary regime (the curves for the stationary regime are not shown in Fig. 3). On the other hand, if the passage begins from the region of strong fields, then the point H^b at which the variation of the field begins lies in this case on the opposite side of the position of H_0^p relative to H^s —accordingly the amplification in the nonstationary regime (dashed) turns out to be much larger in this case than when the field is increased in the same nonstationary regime, or when the field is varied in either direction in the stationary regime. In this case, as seen from Fig. 3a the quantity α_{ns} is increased threefold (and is close to the value of the gain in the absence of detuning, when $\alpha_{ns}(\Delta\nu^s = 0) = \alpha_{st}(\Delta\nu^s = 0)$). We emphasize that under no conditions did the gain in the nonstationary regime exceed the value $\alpha_{st}(\Delta\nu^s = 0)$.

When the sign of the detuning is reversed, i.e., at $\Delta\nu^s = +110$ MHz (Fig. 3a, right side), the situation is correspondingly changed: the gain in the nonstationary regime increases only when the field is increased, i.e., again after passing through the region of the top of the

pump line, inasmuch as the reversal of the sign of $\Delta\nu^s$ is accompanied by change of the relative positions of H_0^p and H^s .

The results of measurements at detunings $\Delta\nu^s = \pm 250$ MHz (Fig. 3b) are even more interesting. In the nonstationary regime, in the case of an “incorrect” choice of the position of H^b as a result of the large detuning (which exceeds the signal-line half-width 32 MHz by almost one order of magnitude) there are not even any symptoms of amplification. Indeed, the solid lines at $\Delta\nu^s = -250$ MHz and the dashed lines at $\Delta\nu^s = +250$ MHz were obtained at maximum pumping, but within the limits of the measurement accuracy (10%) they do not differ from the line of the usual acoustic parametric resonance without pumping. Curves of the same type are obtained also in the stationary regime at $\Delta\nu^s \pm 250$ MHz (the acoustic parametric resonance and the stationary regime are not shown in Fig. 3). If the position of H^b is “correctly” chosen, however (i.e., at $\delta H^s \Delta\nu^s < 0$, $\delta H^p \Delta\nu^s \leq 0$, where $\delta H^s = H^b - H^s$, $\delta H^p = H^b - H_0^p$), an appreciable amplification is obtained with an inversion coefficient $I_{eff} \approx 1$ (at $|\partial H/\partial t| = 200$ Oe/sec). It is quite typical that at $|\partial H/\partial t| = 20$ Oe/sec a distortion of the gain line is observed, due to the decrease of I_{eff} during the course of passage through the signal line, and it is important that the decrease of I_{eff} takes place precisely in the same direction as the variation of the magnetic field. This circumstance makes it possible to estimate directly the nonstationarity time t_{ns} . Besides this method of determining t_{ns} we used also a somewhat different procedure: the magnetic field, initially fixed at the point H^b , was changed in a small step to the value H^s (of course, under conditions when the nonstationary effect took place) and was fixed at the point H^s . The time during which the value of α changed from α_n to α_{st} is precisely t_{ns} . Both methods of measuring the nonstationarity time yielded close results: $t_{ns}(4.2^\circ\text{K}) = 3$ sec and $t_{ns}(1.7^\circ\text{K}) = 10$ sec.

The dependence of the gain on δH^s , measured at $\Delta\nu^s = \pm 250$ MHz, is shown in Fig. 4. The manifestation of the “sign rule” is seen here most clearly: for example, in the case $\Delta\nu^s = -250$ MHz, the gain in the nonstationary regime increases only at $\delta H^s \geq 0$. The maximum values of α_{ns} are reached in this case at $\delta H^s \geq 120$ Oe, which corresponds to $\delta H^p \geq 0$, i.e., to passage of the pump line through the top, when both conditions $\delta H^s \Delta\nu^s < 0$ and $\delta H^p \Delta\nu^s \leq 0$ are satisfied.

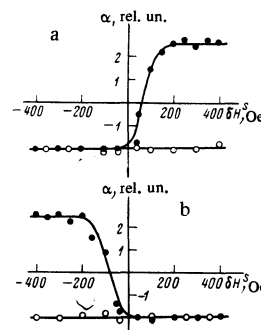


FIG. 4. Plot of hypersound gain against δH^s . Dark points—nonstationary regime ($|\partial H/\partial t| = 200$ Oe/sec); light points—stationary regime ($|\partial H/\partial t| = 2$ Oe/sec). The signal-frequency detuning is $\Delta\nu^s = -250$ MHz (a) and $\Delta\nu^s = +250$ MHz (b).

Besides the experiments described above, which were performed at $\theta = \theta_0$, we have also measured α_{ns} under the following conditions. First, without disturbing the exact tuning with respect to angle $\Delta\theta = \theta - \theta_0 = 0$, we set $\Delta\nu^s = 0$. In this case, naturally, there are no manifestations of the nonstationary effect. Now, however, if detuning with respect to angle is introduced without changing the signal frequency, i. e., $\Delta\nu^s = 0$, then the nonstationary effect appears again in its previous form, that of an increase of α when the magnetic field is varied rapidly in a definite direction, namely, when the condition $\Delta\theta\delta H^s > 0$ is satisfied. The last result can be easily understood by resorting to the level scheme in ruby at $\theta = \theta_0$.^[14] Indeed, at $\Delta\theta > 0$ the resonant pump field (we now have two pump lines instead of one) is stronger than the fixed resonant signal field H_0^s (which corresponds to $\Delta\nu^s = 0$). If we disregard the splitting of the pump resonance, then the situation is similar to the already considered case $\Delta\theta = 0$ and $\Delta\nu^s < 0$. On the other hand, if $\Delta\theta < 0$, the resonant pump fields are weaker than the resonant signal field, and this corresponds to the case $\Delta\theta = \theta$ and $\Delta\nu^s > 0$. Measurements of α_{ns} carried out at $\Delta\theta = \pm(0.5-3^\circ)$ and $\Delta\nu^s = 0$ have confirmed fully the experimental data obtained at $\Delta\theta = 0$ and $\Delta\nu^s \neq 0$.

We measured also the dependence of α on the pump power P under conditions when the relation $\alpha_{ns} \gg \alpha_{st}$ holds at the maximum pumping. We found that a decrease of P leads to a corresponding decrease of the difference $\alpha_{ns} - \alpha_{st}$, and this difference cannot be offset by accelerating the passage, by increasing δH^s , etc.

Thus, saturation of the pump line on the wing, followed by a rapid passage through the region of the pump line vertex, ensures a more effective energy transfer from the pump source (which now saturates the opposite wing) within the limits of the resonance-line contour than in the stationary regime. As a result, the gain of the hypersound signal increases under conditions of strong detuning.

2. The nonstationarity time t_{ns} , as follows from our measurements, exceeds appreciably the spin-lattice relaxation time of the $\text{Cr}^{3+}:\text{Al}_2\text{O}_3$ ions. This circumstance indicates that an important role is played in the nonstationary effect by the system with the small relaxation rate. In ruby this system is made up of the Al^{27} nuclei, the spin-lattice relaxation time τ_n of which, according to NMR measurement data,^[17] is of the same order as t_{ns} at the corresponding concentration and temperature.

It is well known that the Al^{27} nuclear system in ruby is closely coupled with the electron system of the Cr^{3+} ions, because the Zeeman splittings of the nuclear spin levels in fields on the order of several kOe fall in the frequency region of the energy spectrum of the dipole-dipole interaction system of the Cr^{3+} ions. It is also known that induced saturation of the nuclear system, which becomes polarized as a result of the interaction with the electron system, increases the effectiveness of the redistribution of the saturation over the spectrum of the electron system, leading to an acceleration of the cross relaxation^[17,18] and to an increase of the inver-

sion coefficient in the case of detuning in the ordinary electromagnetic ruby maser.^[18,19] The interpretation of the nonstationary effect observed by us will be based on the known concepts concerning the thermodynamics of energy reservoirs produced in this case by the Al^{27} nuclei and the Cr^{3+} ions in ruby.^[17-19]

Let us examine the situation in which the nonstationary effect is realized. At first, when the magnetic field is fixed at the point H^b , the electron system of the pump is saturated under detuning conditions, and this leads, first, to a strong increase of the temperature T_e of the Zeeman electron pool of the pump Z_e in comparison with the temperature T_0 of the lattice, $T_e \gg T_0$, and, second, to polarization of the dipole-dipole interaction pool D_e of the Cr^{3+} ions.^[18] The magnitude and the sign of the polarization $E_D = T_0 T_D^{-1}$ (T_D is the temperature of the pool D_e) are determined by the relative positions of H^b and H_0^p . If the inequality $H^b > H_0^p$ is satisfied, then $E_D > 0$, and vice versa. Detailed measurements have shown^[17] that the nuclear Zeeman pool Z_n of Al^{27} in ruby and the pool D_e are strongly coupled even without the presence of external fields, as a result of which the temperatures of these pools become equalized, i. e., in fact we have $E_n = E_D = E$. The spin-lattice relaxation time of the Al^{27} nuclei at a Cr^{3+} ion concentration 0.03% is quite high at liquid-helium temperatures, $\tau_n(1.9^\circ\text{K}) = 10$ sec.^[17] At the same time, the relaxation of the pool D_e to the pool Z_n is quite rapid, within a time $\tau_{en} < 3 \cdot 10^{-3}$ sec.^[18] This leads to the following conclusion. If the state of the system Z_e is varied rapidly, with the aid of a magnetic field, within a time Δt satisfying the inequality $\tau_{en} \ll \Delta t \ll \tau_n \approx t_{ns}$, then no substantial change will take place in the polarization of the pools D_e and Z_n . Consequently, in experiments with fast passage of the magnetic fields within a time $\Delta t \ll t_{ns}$, i. e., in the nonstationary regime, the polarization of these coupled low-frequency pools can be regarded as constant and specified by the value of δH^p . Taking this circumstance into account, we can easily understand the nature of the nonstationary effect and hypersound amplification.

The value of α is larger the larger T_e . Let us determine T_e as a function of the detuning from the top of the pump line from the kinetic equations that describe our system (Eqs. (15) of^[17]) under the conditions $T_n = T_D = T_0 E^{-1} = \text{const}$ and $w_0 \tau_e \gg 1$, where w_0 is the probability of the induced transition in Z_e under the influence of the microwave field and τ_e is the spin-lattice relaxation time of the Cr^{3+} ions. In this case the solution is obtained in elementary fashion and takes at $t > \tau_e$ the simple form

$$\frac{T}{T_e} \approx -\frac{\Delta}{\nu_0^p} E(H^b), \quad (2)$$

$$\Delta = \nu_0^p - \nu^p.$$

Here ν_0^p is the pump frequency (which corresponds to the field H_0^p), and ν^p is the splitting of the levels of the system Z_e in the field H .

Before we analyze the solution in the nonstationary regime (2), we note that in the stationary regime the condition $T_0 T_e^{-1} \geq 0$ is always satisfied, inasmuch as the stationary nuclear polarization is determined by the mag-

nitude and sign of Δ , with $E\Delta < 0$ always.

In the nonstationary regime, when Δ can vary rapidly, and the polarization of E remains practically constant, owing to the inertia of Z_n , and is governed by the value of δH^b , a situation with $E\Delta > 0$ is possible. We emphasize that in the stationary regime, the last inequality cannot be realized without the action of external sources on Z_n . There are obstacles to obtaining this inequality in the nonstationary regime and, as follows from (2), in this case we have $T_0 T_e^{-1} \lesssim 0$. It is clear that owing to the increase of T_e , up to negative values, the inversion on the signal transition should increase. This, in turn, leads to the increase of α observed in the nonstationary regime. The condition $E\Delta > 0$ is realized only after passing through the top of the pump line, which occurs after a sufficiently prolonged saturation of the wing at $H = H^b$. In fact, after such a prolonged saturation of the wing, a stationary polarization is reached, opposite in sign to Δ (or, equivalently, the sign of the polarization coincides with the sign of δH^b). The passage of the magnetic field through the top of the pump line means a reversal of the sign of Δ , whereas the sign of E remains the same as before during a time $\approx t_{ns}$. As a result, after fast passage through the top we have $E\Delta > 0$, $T_0 T_e^{-1} \lesssim 0$ and $\alpha_{ns} > \alpha_{st}$.

Thus, the increase of the gain of the hypersound in the nonstationary regime is due to the fact that, owing to the reversal of the sign of Δ on going from $\Delta(H^b)$ to $\Delta(H^s)$ through the value $\Delta(H_0^b) = 0$, with the value of $E = E(H^b)$ maintained constant, the temperature of the pump reservoir becomes very high or negative. After E relaxes (within a time t_{ns}) from $E(H^b)$ to $E(H^s)$, the stationary regime is established again.

Since the observed stationary effect is due to the more effective transfer of the saturation within the limits of the electromagnetic-pumping resonance line, it is obvious that this effect takes place also in ordinary electromagnetic masers based on ruby or some other crystal, where the electron dipole pool is strongly coupled with the slowly relaxing system of magnetic nuclei.

5. PHASER EFFECT OF COHERENT PHONON GENERATION

1. With increasing electromagnetic pumping, when the gain of the longitudinal hypersound becomes equal to

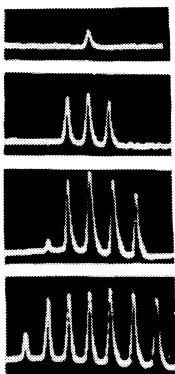


FIG. 5. Spectrum of stationary coherent radiation of phonons at low pump levels. The frequency interval between the neighboring generating modes is 310 kHz. The evolution of the emission spectrum with increasing pump power is shown, starting with the threshold value (downward) $T = 4.2^\circ\text{K}$.

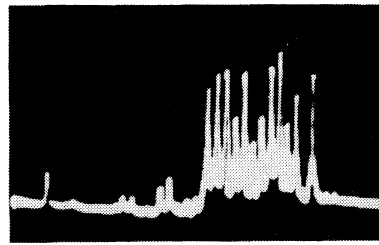


FIG. 6. Emission spectrum in the case of intense pumping (pump power 20 dB above threshold). $T = 1.7^\circ\text{K}$. Spectrum width $B = 8$ MHz.

the absorption of the natural mode in the acoustic resonator, the phonon system becomes self-excited. As a result of the selective amplification of the phonons corresponding to high- Q resonator modes, intense coherent acoustic oscillations set in, and can be directly registered by transforming them with a hypersonic converter into an electromagnetic microwave field. In contrast to other acoustic self-oscillators or microwave electromagnetic generators, the coherent generation is realized in this case simultaneously at many frequencies corresponding to the natural modes of the acoustic resonator.

The radiation at each of these frequencies, which are spaced 310 kHz apart (the frequency difference between the axial longitudinal modes of a ruby resonator 17.6 mm long) is characterized by a narrow spectrum with a relative width less than 10^{-6} . The simultaneity of the generation at several frequencies can be assessed from the narrowness of the spectral lines, and also from the absence of any modulation effects in the observed spectrum. The number of discrete generation frequencies depends on the pump power (Fig. 5). If this power is raised from a value corresponding to the underexcited regime (i. e., to the amplification regime) to the threshold value P_1^1 and above, then single-, three-, five-, etc., frequency generation sets in in sequence. Each of the forms of the $2j+1$ -frequency generation is characterized by its own threshold P_1^{2j+1} . The stationary generation process is established within several strongly-damped oscillations of the intensity of the stimulated emission of the phonons within a time ≈ 1 sec.

This $(2j+1)$ -frequency generation and the increase of the number of generated frequencies with increasing pump are observed only at a relatively slight excess of the pump over P_1^1 (less than 10 dB). At a high pump level, the discreteness of the spectrum is also preserved, but the intensity of the generation and the modes relative to the central mode decreases no longer monotonically: the spectrum becomes chopped up, has dips, etc. (Fig. 6). In addition, besides the principal generating modes, there appear satellites corresponding apparently to not-strictly-axial longitudinal modes (Fig. 7). It is important that the width of the generation spectrum experiences saturation with increasing pump; thus, at a pump 20 dB higher than P_1^1 and at $T = 1.7^\circ\text{K}$, the width of the stimulated-emission spectrum does not exceed 8 MHz, which is much narrower than the above-threshold region of the gain line. A width of the same order is observed in the phaser-generation spectrum

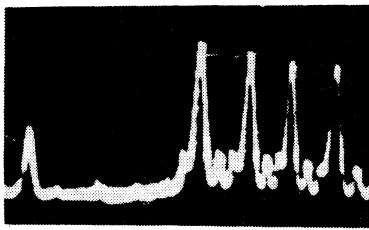


FIG. 7. Satellites in phonon coherent-emission spectrum in the gap between the frequencies of the fundamental modes (intense pumping), $T = 4.2^\circ\text{K}$.

also at $T = 4.2^\circ\text{K}$. The emission intensity at each of these frequencies, after the corresponding modes begin to generate, first increases with increasing pump, but then exhibits saturation, reaching a value on the order of several $\mu\text{W}/\text{cm}^2$. The integrated intensity of the stimulated hypersonic emission in the crystal reaches $\approx 100 \mu\text{W}/\text{cm}^2$.

2. Let us discuss the mechanism of multifrequency generation of the phaser. Obviously, just as in any self-oscillator, multifrequency stationary generation is possible in a phaser only in the presence of a large number of weakly-coupled self-oscillating systems with stable limit cycles. The explanation of the mechanism of phaser generation is therefore directly connected with the possibility of separating, in an acoustic resonator with impurity centers, a number of weakly coupled self-oscillating systems with different frequencies. The solution of this problem is facilitated by the fact that a similar question was considered earlier in the study of the cause of multimode generation of lasers.

According to [20], multimode generation is stable in the case of weak coupling, when the width of the homogeneous resonance lines is less than the frequency interval between the neighboring modes of the hypersonic resonator. In this case generation takes place under conditions of spectral disequilibrium (in terms of the kinetic theory of lasers [21]), when the spin packets that contribute to generation have different frequencies. The feasibility of realizing such a narrow homogeneous line is based on the following. In magnetically-dilute crystals, including ruby, the linewidth $\langle\Delta\nu\rangle_p$ is essentially inhomogeneous and is determined by the scatter of the crystal-field parameters. If it is assumed that the homogeneous broadening is definitely a microscopic effect, when the neighboring spins differ in their resonant frequencies, then it is easy to show that the homogeneous linewidth $\langle\Delta\nu\rangle_0$ is of the order of $\langle\Delta\nu\rangle^2\langle\Delta\nu\rangle_p^{-1}$. [22] Here $\langle\Delta\nu\rangle^2$ is the second moment of the line and is due to the dipole-dipole interactions. Since $\langle\Delta\nu\rangle \ll \langle\Delta\nu\rangle_p$, the homogeneous line width is in this case much smaller than the dipole-dipole width and satisfies the condition stated above.

Another possible interpretation of the multifrequency generation, without invoking the assumption that the inhomogeneous broadening is of microscopic origin, is to consider the generation under conditions of spatial disequilibrium, i. e., when the excitations are spatially separated. On this basis it is possible to describe

qualitatively the main features of the observed phaser generation.

A hypersonic resonator is an oscillating system with a large number of degrees of freedom, and consequently admits of the formation of weakly-coupled excitations even under conditions when the homogeneous line width exceeds the frequency difference between the neighboring modes. The point is that the elastic field of the generating modes in the resonator is essentially inhomogeneous and can be represented in the form of a superposition of standing waves, the number of which is equal to the number of generating modes. As a result of the low rate of spatial migration of the excitations, the impurity centers located in the antinodes of the standing waves, corresponding to different resonator modes, participate independently in the generation at frequencies corresponding to these modes.

From an analysis of the rate equations for the 4-level spin system of ruby, it is easy to show that the inverted difference of the populations \bar{m} of the signal transition, just as for the ordinary laser scheme, can be represented in the form [23, 24]

$$\bar{n} = \bar{n}_0 \left(1 + D \sum_i p_i g_i \right)^{-1}, \quad p_i = N_i [1 - \cos(2\pi m_i z/L)],$$

where g_i is the ordinate of the resonance line at the frequency of the i -th mode, L is the length of the resonator, m_i are integers, N_i is the number of phonons in the i -mode, D is a quantity proportional to the probability of the induced radiation, \bar{n}_0 is the difference of the populations in the absence of radiation, and z is the coordinate along the resonator axis.

In this case, the laser conditions for stationary ($2j + 1$)-mode generation remain in force for the phaser, as does the limiting width of the spectrum B [24]

$$\bar{\alpha} = \frac{(1 + \beta j^2)^2}{1 - \beta j (8j^2 - 3j - 2)}, \quad B = 1.4 \beta^{-1} \delta\nu, \quad \bar{\alpha} = \bar{n}_0/n_0^t, \quad \beta = (\delta\nu/\Delta\nu)^2. \quad (3)$$

Here \bar{n}_0^t is the threshold population difference; $\delta\nu$ is the distance between the frequencies of the neighboring modes, and $\Delta\nu$ is half the width of the resonance line of the signal transition.

The experimental data shown in Fig. 8 reveal a qualitative agreement with (3). With increasing pump, \bar{n}_0 increases, and $\bar{\alpha}$ with it, and this leads to a jumplike increase in the number of modes that begin to generate. It follows from (3) that the limiting width of the spectrum at $\Delta\nu = 32 \text{ MHz}$ and $\delta\nu = 310 \text{ kHz}$, i. e., at $\beta = 10^{-4}$,

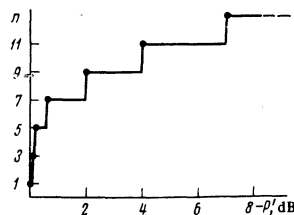


FIG. 8. Dependence of the number $n = 2j + 1$ of modes that go into generation on the pump power $T = 4.2^\circ\text{K}$, $P' = 10 \log(P/P_t)$, $P_t = 10^{-4} \text{ W}$.

is equal to 9 MHz, which is also in good agreement with the measured $B=8$ MHz.

The considered mechanism of phaser generation under conditions of spatial disequilibrium corresponds to a monotonic decrease of the spectrum intensity with increasing distance from the center of the resonance lines. This monotonic decrease, as noted above, is observed only at small excesses above the generation threshold. The fact that the decrease is no longer monotonic at high pump levels (Figs. 6 and 7) demonstrates the limited character of this analysis. The irregularities and the dips in the spectrum show that at high pump levels the resonance line acquires a fine structure which apparently leads to the aforementioned spectral disequilibrium, when individual regions of lines that are quite close in frequency make independent contributions to the generation.

The authors thank M. S. Soskin, useful discussions with whom helped determined the coherent-phonon generation mechanism, and also N. L. Kenigsberg for preparing the zinc-oxide films for the hypersonic converters.

¹Brief reports of some results of this work were published earlier.^{9,10}

²In the pulsed measurements, the resonant properties of the rod can be disregarded, since $\tau\nu < l_0$ (τ is the pulse duration and l_0 is the length of the rod).

¹C. H. Townes, Quantum Electronics, Proc. First Conf., ed. C. H. Townes, Columbia Univ. Press, N. Y., 1960, p. 405.

²U. Kh. Kopvillem and V. D. Korepanov, Zh. Eksp. Teor. Fiz. 41, 211 (1961) [Sov. Phys. JETP 14, 154 (1962)].

³C. Kittel, Phys. Rev. Lett. 6, 449 (1961).

⁴E. B. Tucker, *ibid.*, 547.

⁵E. B. Tucker, Quantum Electronics, Proc. Third Conf., ed. P. Grivet and N. Blomebergen, vol. 2, Columbia Univ. Press, 1964, p. 1787.

⁶P. D. Peterson and E. H. Jacobsen, Science 164, 1065

(1969).

⁷G. Makhov, L. G. Cross, R. W. Terhune, and J. Lambe, J. Appl. Phys. 31, 936 (1960).

⁸K. J. Standley, G. D. Adam, W. S. Moore, and B. E. Storey, Magnetic and Electric Resonance and Relaxation, Proc. Eleventh Ampere Colloquium, ed. J. Smidt, Amsterdam, 1963, p. 535.

⁹E. M. Ganapol'skiĭ and D. N. Makovetskiĭ, Dokl. Akad. Nauk SSSR 217, 303 (1974) [Sov. Phys. Dokl. 19, 432 (1975)].

¹⁰E. M. Ganapol'skiĭ and D. N. Makovetskiĭ, Solid State Commun. 15, 1249 (1974).

¹¹E. M. Ganapol'skiĭ, Prib. Tekh. Eksp. 6, 214 (1969); Fiz. Tverd. Tela (Leningrad) 12, 2606 (1970) [Sov. Phys. Solid State 12, 2095 (1971)].

¹²E. M. Ganapol'skiĭ and D. N. Makovetskiĭ, Fiz. Tverd. Tela (Leningrad) 15, 2447 (1973) [Sov. Phys. Solid State 15, 1625 (1974)].

¹³S. A. Al'tshuler and B. M. Kozyrev, Elektronnyi paramagnitnyi rezonans (Electron Paramagnetic Resonance), Nauka, 1972, p. 283.

¹⁴A. E. Siegmann, Introduction to Masers and Lasers, McGraw, 1971 (Russ. transl., Mir, Appendix).

¹⁵V. B. Shteĭnshleĭger, G. S. Mizezhnikov, and P. S. Lifanov, Kvantovye usiliteli SVCh (Microwave Quantum Amplifiers), Sov. Radio, 1971, Chap. 2.

¹⁶C. Jeffries, transl. in: Dinamicheskaya orientatsiya yader (Dynamic Orientation of Nuclei), Mir, 1965, p. 69.

¹⁷V. A. Atsarkin, A. E. Mefed, and M. I. Rodak, Zh. Eksp. Teor. Fiz. 55, 1671 (1968) [Sov. Phys. JETP 28, 877 (1969)].

¹⁸V. A. Atsarkin and M. I. Rodak, Usp. Fiz. Nauk 107, 3 (1972) [Sov. Phys. Usp. 15, 251 (1972)].

¹⁹V. A. Atsarkin, Fiz. Tverd. Tela (Leningrad) 12, 1775 (1970) [Sov. Phys. Solid State 12, 1405 (1970)].

²⁰W. E. Lambe, Jr., Phys. Rev. 134, A1429 (1964).

²¹V. S. Mashkevich, Kineticheskaya teoriya lazerov (Kinetic Theory of Lasers), Nauka, 1971.

²²N. Bloembergen, S. Shapiro, P. S. Pershan, and J. O. Artman, Phys. Rev. 114, 445 (1959).

²³C. L. Tang, H. Statz, and G. deMars, J. Appl. Phys. 34, 2289 (1963).

²⁴B. L. Lifshitz and V. N. Tsikunov, Zh. Eksp. Teor. Fiz. 49, 1843 (1965) [Sov. Phys. JETP 22, 1260 (1966)].

Translated by J. G. Adashko

Dynamic damping of dislocations in ferromagnets

V. G. Bar'yakhtar and E. I. Druinskiĭ

Khar'kov Physico-technical Institute, Ukrainian Academy of Sciences

(Submitted June 10, 1976)

Zh. Eksp. Teor. Fiz. 72, 218-224 (January 1977)

Dynamic damping of dislocations by spin waves in ferromagnets is investigated. The dependence of the magnon damping force on temperature and velocity is calculated. A general picture is presented of the temperature dependence of the dynamic damping force on dislocations in ferromagnets.

PACS numbers: 75.30.Ds, 61.70.Ga

INTRODUCTION

Motion of dislocations in a crystal, which causes the process of plastic deformation, is limited, as is well known (see, for example,^[1]), by two qualitatively different phenomena: the surmounting of barriers through

fluctuations, and dynamic damping caused by scattering of the energy of a dislocation by elementary excitations in the crystals (phonons, electrons, spin waves, etc.). Because of the fact that the density of an elementary-excitation gas increases with rise of temperature (electrons in a normal metal are an exception), the contribu-